Journal of Basic and Environmental Sciences

ISSN
Online:2356-6388
Print:2536-9202

Research Paper Open Access

Preparation and characterization $ZnMn_2O_4$ via auto-combustion synthesis

I. H. Ahmed, A. A. Ali, M. M. Elsayed, A. M. El-sharkwy, S. A. Shama

Chemistry Department, Faculty of science, Benha University, Benha, Egypt

Email:drislam992021@gmail.com Tele: 00201000386556

Abstract

$ZnMn_2O_4$ nanoparticles were synthesized by combustion method using urea and glycine fuels. $ZnMn_2O_4$ nanoparticles studied using XRD, FTIR, and DRS tools. The crystallize size determined by XRD to was about 16 nm. The direct band gap determined by using the extracted data from DRS. The obtained $ZnMn_2O_4$ nanoparticles were used for the removal of the conge red dye from aqueous media.

Keywords: $ZnMn_2O_4$ nanoparticles, Combustion method, Band gap, Conge red dye.

1. Introduction

Environmental issues have become contentious among researchers, especially the concern on water pollution. Clean water is reduced due to increasing of industrialization. The dyes and phenolic compounds are organic pollutants that cause environmental contamination, especially to water pollution and are also harmful to the human body [1-4]. The source that polluted water must be removed rapidly. There are some ways to remove pollution from aqueous solutions depend on the source and the type of pollution, including chemical oxidation ion exchange, membrane separation, electro chemical techniques, adsorption and photo catalysis [5]. The adsorption is one method for the removal dye pollutant from water,this way is considered as one of the important and efficient approaches to dismiss the dyes in wastewater. While most organic materials such as dyes are the common pollutants in wastewater of some industries like food, textiles and pharmaceuticals. The problem is directed due to the carcinogenicity and

mutagenicity of these non-biodegradable and highly toxic chemical substances [6].

Nanosized metal oxides are present in different forms, such as particles, tubes and spherical shape and others. The size and shape of nanomaterials are both important factors to affect their adsorption performance. Efficient synthetic methods to obtain shape-controlled, monodisperse , and highly stable metal oxide nanomaterials have been widely studied during the last decade. The corresponding preparation methods may be grouped in two main streams based upon the liquid-solid and gas solid nature of the transformations. Liquid-solid transformations are possibly the most broadly used to control morphological characteristics with certain chemical versatility [7-9]. A few specific methods have been developed, among which those broadly in use in the preparation of nanomaterials such as combustion, sol-gel, hydrothermal and other methods[10-15]. In this Research, $ZnMn_2O_4$ nanoparticles prepared using a combustion method following by the calcination was adopted. The obtained materials are characterized by using different tools and used av photo catalyst for the removal of an organic dye.

2.Experimental

2.1. Materials and reagents

All chemicals used in this work were purchased and used as received without any further purification: Zinc nitrate $Zn(NO_3)_2.6H_2O$ (98%), Manganese acetate $Mn(CH_3COO_2)_2.H_2O$ (98%), conge red, Hydrogen Peroxide (H_2O_2, 30%), urea, glycine were purchased from Sigma-Aldrich Company.

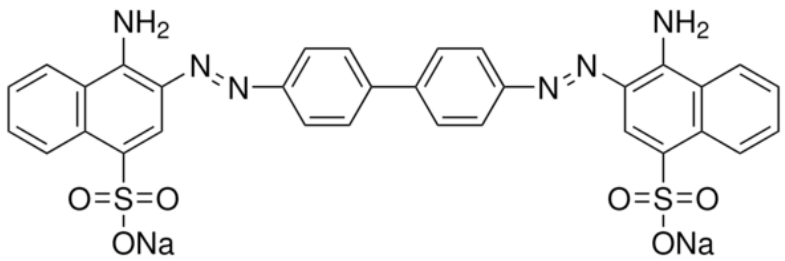

Figure (1) the chemical structure of conge red dye.

2.2. Preparation of $ZnMn_2O_4$ via combustion method:

Zinc nitrate, Manganese acetate, urea and glycine were dissolved in 50 mL deionized water under stirring to get homogenous solution. The solution heated on hot plate until auto-ignition was finished at the release of gases and gray ash was obtained. The as-synthesized ashes were transferred into furnace and calcined at 500°C for one hour to remove residual organic materials.

2.3. Photocatalytic measurements

The Congo dye used as acontaminant to investigate the photocatalytic property of $ZnMn_2O_4$. 50 mg of photo catalyst were weighted and used to accelerate the dye degradation reaction. In this study, concentration and volume of dye solutions used were 30 ppm and 50 mL, respectively. The photo catalytic experiments were studied under UV-irradiation (Philips UV-mercury lambs (365 nm). The suspension, containing dye photo catalyst, we aerated in darkness and stirred different times. The suspension was sampled and centrifuged to remove the remained photo catalysts of the dye solution. Then absorbance spectrum of the solution was recorded, and photo degradation efficiency using the below equation was estimated as showed in eq. (1). Ao and A are absorbance quantities of dye solution before and after degradation, respectively. Kinetic studies of the photo degradation of the testing dyes over the fabricated sample was tested using frst-order models as represented in eq. (2) [16].

$$\boldsymbol{Degradation}\,\% = \left|\frac{\boldsymbol{A_0 - A}}{\boldsymbol{A_0}}\right| \boldsymbol{x100} \qquad (\mathbf{1})$$

$$\boldsymbol{Ln}(\,\boldsymbol{C_0}\,/\,\boldsymbol{C_t}\,) = \boldsymbol{Kt} \qquad (\mathbf{2})$$

2.4. Characterization:

The X-ray diffraction is employed to examine the structure of nanoparticles using diffractometer (Bruker; model D8 advance) with monochromatic Cu-Kα irradiation. The as-prepared samples were measured using FTIR spectrometer at room temperature from 4000 to 400 cm^{-1}. Calcined sample's diffuse reflectance was investigated in ultraviolet-visible NIR range (200-2500 nm) using Jasco-V670 spectrophotometer where the integrating sphere calibrated with barium sulfate as white standard was used.

3. Result and Discussion:

3.1. XRD study

Figure (2) shows XRD pattern of the products prepared from salts of metals via combustion method followed by the calcination at 500 ^{o}C for one hour. The obtained product is pure $ZnMn_2O_4$ according to card no. JCPDS No. 01–077–0470 [17]. The diffraction peaks in this figure (2) are matched those of the standard tetragonal spinel phase $ZnMn_2O_4$. These peaks at 2-theta values, intensity and d values are shown in Table 1. The average particle size of $ZnMn_2O_4$ sample was calculated to be 16 nm, by the Scherrer equation [18], by using the X-ray line broadening analysis of the main diffraction line of

this sample as represented in Eq No 3.

$$D = K\lambda / \beta \cos \theta \qquad (3)$$

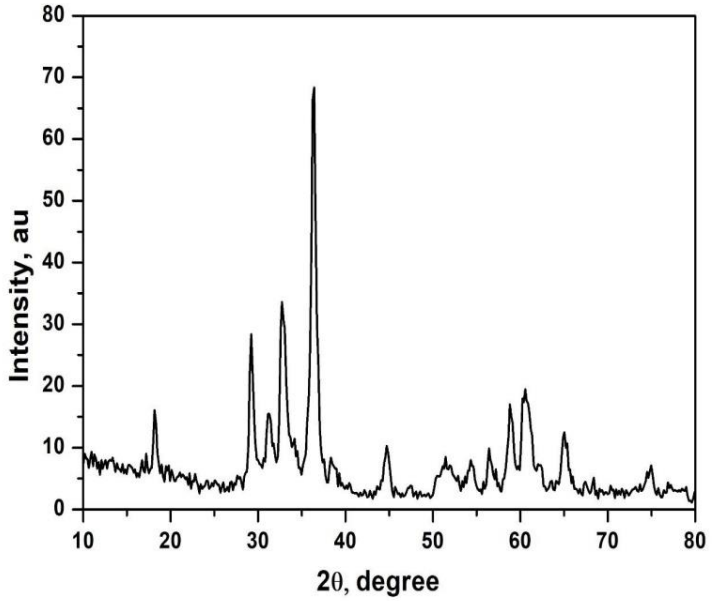

Figure (2) XRD pattern of the synthesized $ZnMn_2O_4$ nanoparticles using the combustion method.

Table (1)

The peaks, intensity, d and two theta values of the synthesized ZnMn2O4 nanoparticles.

Caption	Angle, 2-Theta °	d value, Angstrom	Intensity, Count	Intensity %
d=4.85497	18.259	4.85497	12.8	17.7
d=3.04958	29.262	3.04958	27.8	38.5
d=2.86081	31.24	2.86081	15.7	21.8
d=2.73021	32.776	2.73021	33.3	46.2
d=2.46659	36.395	2.46659	72.1	100
d=2.32527	38.692	2.32527	7.47	10.4
d=2.01868	44.864	2.01868	10.6	14.7
d=1.75883	51.948	1.75883	8.65	12
d=1.68360	54.456	1.6836	7.86	10.9
d=1.62655	56.534	1.62655	9.83	13.6
d=1.56626	58.919	1.56626	18.3	25.4
d=1.52909	60.499	1.52909	19.3	26.7
d=1.43387	64.989	1.43387	12.6	17.5
d=1.26817	74.805	1.26817	7.47	10.4

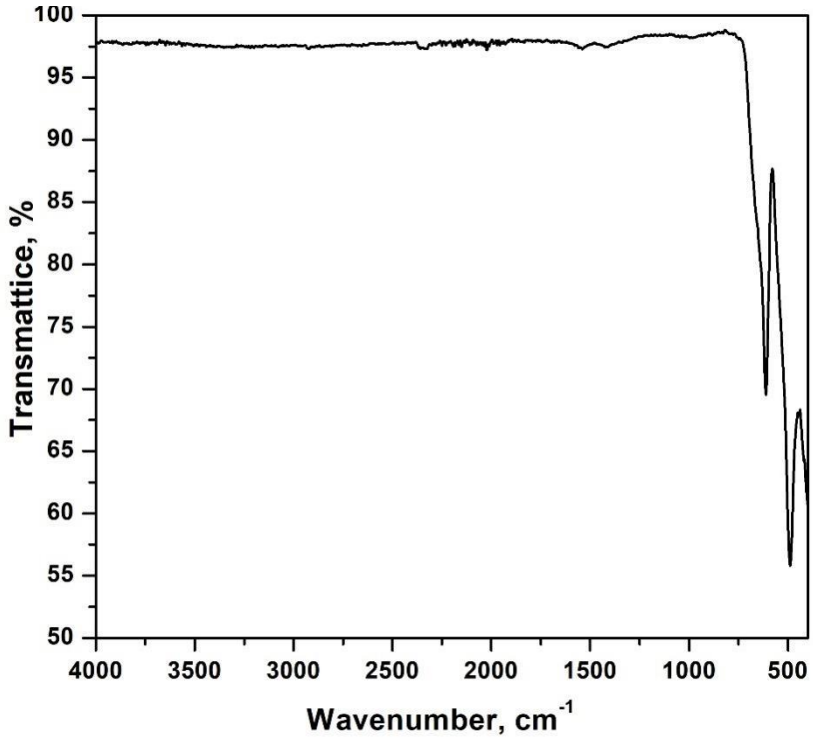

Figure (3) FTIR of the synthesized $ZnMn_2O_4$ nanoparticles using combustion method.

3.2. FT-IR study

Figure (3) shows the FTIR spectra of the synthesized $ZnMn_2O_4$ nanoparticles after the calcination at 500 ^oC for 1 hour. Peaks at 500 and 600 cm^{-1} are related to the $ZnMn_2O_4$ spinel structure [1, 17]. The vibration peaks recorded in the range of 400-600 cm^{-1} are related to Mn—O—Zn, Zn —O and Mn—O bonds.

3.3. Optical properties

The synthesized $ZnMn_2O_4$ sample investigated using UV-Vis and NIR diffuse reflectance and absorbance spectra as shown in Figure 4(a and b). Kubelka Munk function is written by Eq. No. 4. The spectra shows the small reflectance edge at 500 nm for $ZnMn_2O_4$ sample as shown in Figure 4(b). Spectra of $ZnMn_2O_4$ nanoparticles show the broad absorption band between 250-650 nm with heads at 450 nm as shown in figure 4(b).

$$\mathbf{F(RE) = (1 - RE)^2/2RE} \qquad (4)$$

Where RE is the reflectance data of the calcined sample and F(RE) is Kubelka Munk function. The direct and indirect band gap of the prepared powder can be determined by using Eq. No. 5.

$$\mathbf{(F(RE)h\upsilon)^M = S(h\upsilon - E_g)} \qquad (5)$$

Where F(RE) is Kubelka Munk function, F($h\upsilon$) is energy function, R is the reflectance of the samples, S is constant and M is the value between 2 and 1/2

based on the direct and indirect allowed electronic transitions, respectively. The direct and indirect allowed electronic transitions band gap of the prepared powder can be determined by using the equation (5) to be 1.8 eV, 1.5 eV, respectively as shown in Figure 4(c and d).

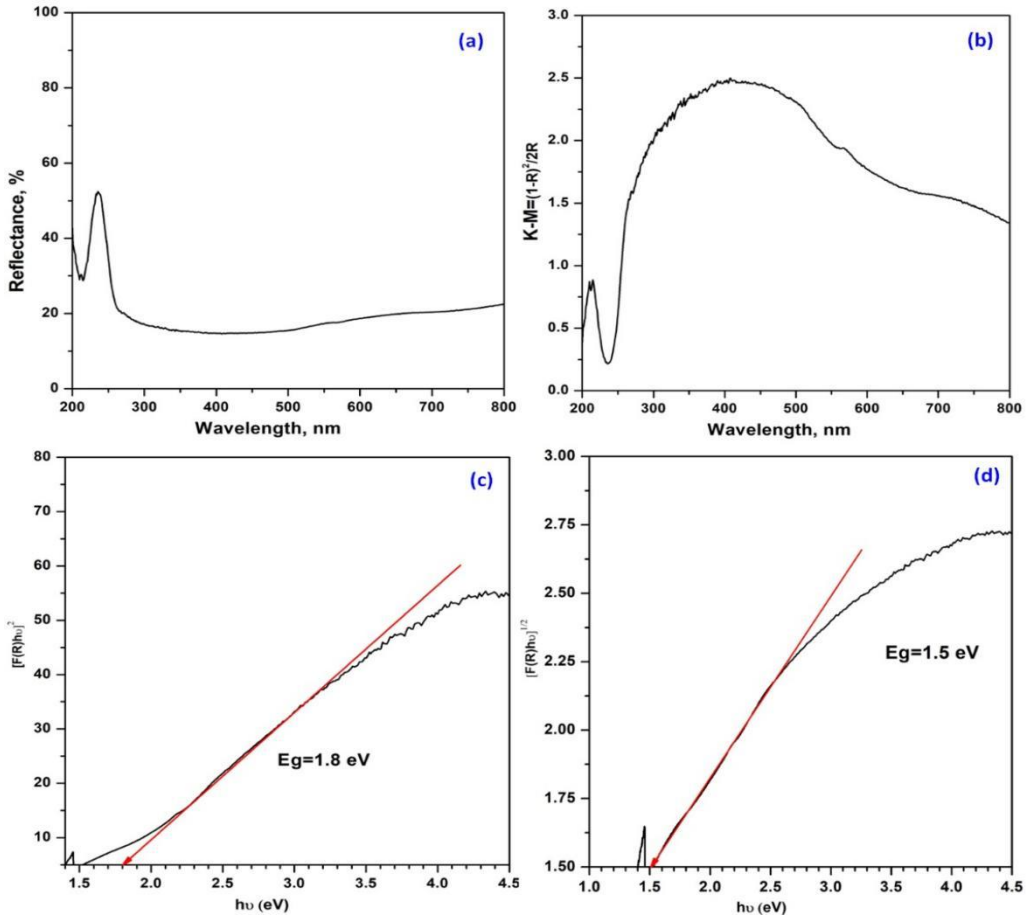

Figure (4) Diffuse reflectance (a), UV-Vis spectra, UV-Vis absorption spectra (b), (c) direct and (d) indirect band gap of the synthesized $ZnMn_2O_4$ nanoparticles.

3.3. Photocatalytic properties

The photocatalyst degradation of conge red dye was studied using $ZnMn_2O_4$ nanoparticles as shown in Figure (5). The photocatalytic degradation of the dye is studied. The degradation percentage, R^2 values and rate constant (K, min^{-1}) of degradation of conge red dye using $ZnMn_2O_4$ are summarized in Table (2) with and without the presence of H_2O_2. The degradation of conge dye with and without H_2O_2 reached about 72%, 55% after 80 min and 120 min irradiation, respectively. Figure 5(c and d) showed the kinetic model in the form of the First order model of the degradation of conge red (C R) under UV-light over $ZnMn_2O_4$. The rate of degradation of C R dye over $ZnMn_2O_4$ in the presence of H_2O_2 (80 min) is faster than without H_2O_2 in 120 min [19, 20].

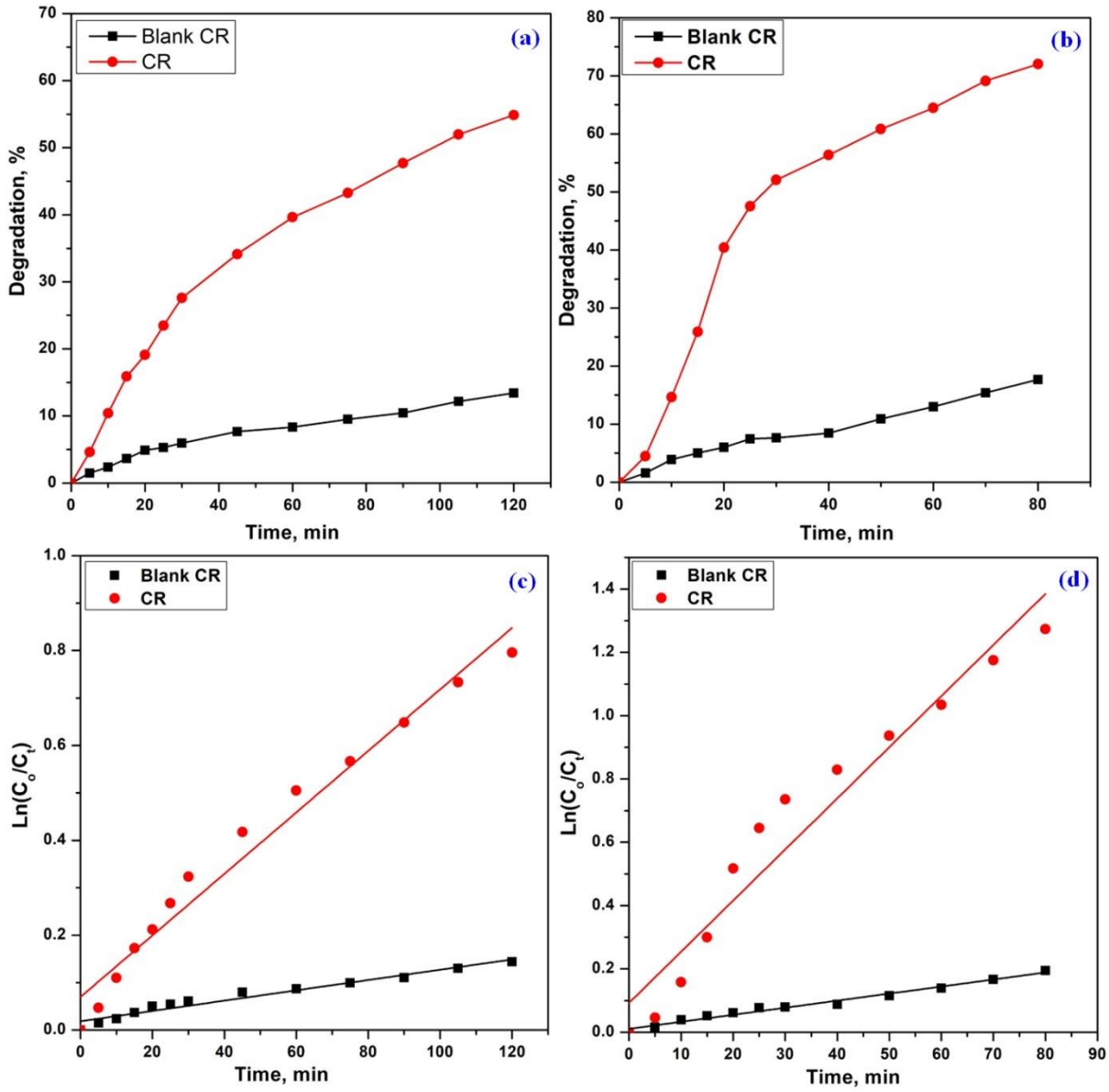

Figure (5) photocatalytic degradation and kinetic of conge red dye on $ZnMn_2O_4$ nanoparticles with (a, c) and without (b, d) H_2O_2, respectively.

Table (2)
Kinetic of the degradation of conge red dye on $ZnMn_2O_4$ nanoparticles (First order model)

Type of order		With H_2O_2	Without H_2O_2
First order model	K, min^{-1}	0.0162	0.0065
	R^2	0.944	0.974
	D, %	72	55

4.Conclusions:

$ZnMn_2O_4$ nanoparticles were synthesized by combustion method using urea and glycine fuels. $ZnMn_2O_4$ nanoparticles studied using different tools. The crystallize size determined by XRD was 16 nm. The direct and indirect band gap determined was 1.8 and 1.54 eV. The obtained $ZnMn_2O_4$ nanoparticles were used for the removal of the conge red dye from aqueous media. The photocatalyst degradation of conge red dye using $ZnMn_2O_4$ nanoparticles was determined to be 55% and 72% in the absence and presence of H_2O_2 respectively.

Reference:

[1] A. Sobhani, S. Alinavaz, ZnMn2O4 nanostructures: Synthesis via two different chemical methods, characterization, and photocatalytic applications for the degradation of new dyes, Heliyon, 9 (2023) e21979.

[2] A.A.S. Ali, Sayed A Amin, Alaa S EL-Sayed, Sahar R, Synthesis and characterization of ZrO_2/CeO_2 nanocomposites for efficient removal of Acid Green 1 dye from aqueous solution, Mater. Sci. Eng., B, 269 (2021) 115167.

[3] A.A. Ali, S.R. El-Sayed, S.A. Shama, T.Y. Mohamed, A.S. Amin, Fabrication and characterization of cerium oxide nanoparticles for the removal of naphthol green B dye, Desalination and Water Treatment, 204 (2020) 124-135.

[4] A. Ali, H. Aly, I. Ahmed, F. Fathi, Sol-Gel Auto-Combustion Preparation and Characterization of Silica Nanoparticles for The Removal of Congo Red Dye from Aqueous Media, J Benha Journal of Applied Sciences, 5 (2020) 199-208.

[5] H. G Fouad, A. S Amin, I. S Ahmed, A. A Ali, Zinc-aluminium layered double hydroxides: Fabrication, study and adsorption application for removal organic dye from aqueous media, Benha Journal of Applied Sciences, 7 (2022) 53-61.

[6] P.O. Oladoye, M.O. Bamigboye, O.D. Ogunbiyi, M.T. Akano, Toxicity and decontamination strategies of Congo red dye, Groundwater for Sustainable Development, 19 (2022) 100844.

[7] I. Ahmed, S. Shama, H. Dessouki, A. Ali, Low temperature combustion synthesis of CoxMg1−xAl2O4 nano pigments using oxalyldihydrazide as a fuel, Mater. Chem. Phys., 125 (2011) 326-333.

[8] I.S. Ahmed, S.A. Shama, H.A. Dessouki, A.A. Ali, Synthesis, thermal and spectral characterization of nanosized NixMg1−xAl2O4 powders as new ceramic pigments via combustion route using 3-methylpyrozole-5-one as fuel, Spectrochim. Acta, Part A, 81 (2011) 324-333.

[9] I. Ahmed, H. Dessouki, A. Ali, Synthesis and characterization of NixMg1− xAl2O4 nano ceramic pigments via a combustion route, Polyhedron, 30 (2011) 584-591.

[10] A.A. Ali, I.S. Ahmed, A.S. Amin, M.M. Gneidy, Preparation, characterization and optical properties of copper oxide nanoparticles via auto-combustion method.

[11] A.A. Ali, M.Y. Nassar, M. Abd Elazeem, I.S. Ahmed, M. Abd, E.J.B.E.S. Abd Elhalim, Fabrication and study of Nickel oxide nanoparticles via low combustion synthesis method using different fuels, 6 (2019) 183-186.

[12] A. Ali, E. El Fadaly, I. Ahmed, Near-infrared reflecting blue inorganic nano-pigment based on cobalt aluminate spinel via combustion synthesis method, Dyes and Pigments, 158 (2018) 451-462.

[13] A.A. Ali, I.S. Ahmed, Sol-gel auto-combustion fabrication and optical properties of cobalt orthosilicate: Utilization as coloring agent in polymer and ceramic, Mater. Chem. Phys., 238 (2019) 121888.

[14] A.A. Ali, S.A. Shama, S.R. EL-Sayed, Fabrication, structural and adsorption studies of zirconium oxide nanoparticles, J Benha Journal of Applied Sciences, 5 (2020) 245-253.
[15] I. Ahmed, H. Dessouki, A. Ali, Synthesis and characterization of new nano-particles as blue ceramic pigment, Spectrochim. Acta, Part A, 71 (2008) 616-620.
[16] A.A. Ali, I.S. Ahmed, A.S. Amin, M.M. Gneidy, Auto-combustion Fabrication and Optical Properties of Zinc Oxide Nanoparticles for Degradation of Reactive Red 195 and Methyl Orange Dyes, J. Inorg. Organomet. Polym Mater., 31 (2021) 3780-3792.
[17] K.-x. Cai, S.-h. Luo, J. Cong, K. Li, S.-x. Yan, P.-q. Hou, Q. Wang, Y.-h. Zhang, X. Liu, Enhancement of lithium storage performance of ZnMn2O4 anode by optimizing hydrothermal synthesis, Transactions of Nonferrous Metals Society of China, 33 (2023) 2772-2783.
[18] A. S Mohamed, L. Abdelhafez, S. Shama, A. Ali, Fabrication, study, and optical properties of zinc ferrite using combustion method and glycine, Benha Journal of Applied Sciences, 7 (2022) 143-148.
[19] A.A. Ali, E.A. El Fadaly, N.M. Deraz, Auto-combustion fabrication, structural, morphological and photocatalytic activity of CuO/ZnO/MgO nanocomposites, Mater. Chem. Phys., 270 (2021) 124762.
[20] M.Y. Nassar, A.A. Ali, A.S. Amin, A facile Pechini sol–gel synthesis of TiO2/Zn2TiO2/ZnO/C nanocomposite: an efficient catalyst for the photocatalytic degradation of Orange G textile dye, RSC Adv., 7 (2017) 30411-30421.